PHYSICAL REVIEW B

SOLID STATE

THIRD SERIES, VOL. 3, NO. 2 15 JANUARY 1971

Doppler-Shifted Open-Orbit Resonance and High-Field Magnetoacoustic Oscillations in Ultrapure Copper†

W. Royall Cox and J. D. Gavenda
Department of Physics, The University of Texas, Austin, Texas 78712
(Received 29 June 1970)

Doppler-shifted open-orbit resonance and high-field magnetoacoustic oscillations have been observed in ultrapure copper at 4.2 °K with compressional sound waves propagating along the [$\bar{1}$01] axis. A Doppler-like splitting of the resonance peak associated with the [010]-directed open orbits begins when $\vec{B}$ is rotated about 0.1° away from [101] in the ($\bar{1}$01) plane and increases in magnitude with rotation angle. From the splitting one can deduce average cyclotron masses, which exceed the free-electron mass by as much as a factor of 30, and average drift velocities, which are one hundred times smaller than the free-electron Fermi velocity. Magnetoacoustic oscillations caused by extended orbits along the [010]- and [111]-directed open-orbit bands were studied in fields up to 27 kG, and orbits covering as many as sixty Brillouin zones were measured. All experimental results are compared with the model Fermi surface proposed by Halse.

I. INTRODUCTION

Open orbits are known[1] to be very important in determining the transport properties of metals, and investigations[2] of electrons on such orbits have contributed much to the understanding of these properties. The purpose of this paper is to report the observation of two effects caused by open orbits in copper which appear in the ultrasonic attenuation data: Doppler-shifted open-orbit resonance and high-field magnetoacoustic oscillations. The first effect provides quantitative information about cyclotron masses and electron drift velocities, while the second can be of importance in the interpretation of high-field attenuation data. A detailed analysis is made of these phenomena using compressional waves in a single crystal of copper[3] having a residual resistivity ratio of 35 000 at a temperature of 4.2 °K.

The fact that electrons moving on open trajectories in a direction perpendicular to an applied magnetic field can absorb energy resonantly from a sound wave was first discussed by Galkin, Kaner, and Korolyuk.[4] Such resonances occur when the projection of the $\vec{r}$-space orbit period along the direction of sound propagation is equal to an integral number of wavelengths. A Doppler splitting of the resonance peak can be observed when the component of the average velocity of the open-orbit electrons along the sound-wave propagation direction does not exceed the sound velocity by more than about one order of magnitude. If the magnetic field is not exactly perpendicular to the open direction, and if the electron mean free path is long enough, then the open orbits eventually coalesce into elongated closed orbits which can extend over many Brillouin zones. The matching of these extended orbits in $\vec{r}$ space to the sound wavelength then gives rise to magnetoacoustic (geometric)-type oscillations at high magnetic fields.

Open-orbit resonances have been observed in copper[5,6] and several other[2] metals, and magnetoacoustic oscillations due to extended orbits have been seen at relatively low magnetic fields in cadmium.[7,8] However, only in gallium[9] was a Doppler effect seen, and no magnetoacoustic oscillations have been reported for any metal at *high* fields (where the electron cyclotron radius for single-zone orbits is much less than a wavelength of sound). The Fermi surface of copper supports open orbits in many[10] directions, but this work is confined to a study of the "primary" open-orbit band along ⟨111⟩ and a "secondary" band along ⟨010⟩. The relative orientations and widths

of these bands are indicated in Fig. 1.

II. THEORY

The electronic attenuation of a compressional sound wave propagating through a pure crystal along an axis of high symmetry may be expressed quite generally in the form[2]

$$\alpha \propto \mathrm{Re} \sum_{n=-\infty}^{\infty} \int \frac{F_n(k_z, \omega_c, \vec{q}, \vec{D})\, dk_z}{\langle \tau^{-1} \rangle + i(\vec{q} \cdot \langle \vec{v} \rangle - \omega - n\omega_c)} \ . \qquad (1)$$

The magnetoacoustic-oscillation effects are contained in the real function $F_n(k_z, \omega_c, \vec{q}, \vec{D})$, which involves an integration around the orbit in each k_z plane perpendicular to $\vec{B}$ and depends upon the cyclotron frequency ω_c, the sound-wave propagation vector $\vec{q}$, and the deformation parameter $\vec{D}$. Resonance effects from the imaginary part of the denominator in Eq. (1) can appear in α if the relaxation time τ is large. The condition for Doppler-shifted open-orbit resonance is similar to that for acoustic cyclotron resonance and may be expressed in the form

$$|\vec{q} \cdot \langle \vec{v} \rangle - \omega| = n\omega_c, \quad n = 1, 2, \ldots \qquad (2)$$

where $\langle \vec{v} \rangle$ is the electron velocity averaged over a period of motion in the magnetic field. It is seen from Eq. (2) that electrons drifting in opposite directions along $\vec{q}$ come into resonance with the sound wave at slightly different series of magnetic field values:

$$B_n^{\pm} = (cqm_c/ne)(\langle v_q \rangle \pm v_s) \ . \qquad (3)$$

Here $\langle v_q \rangle$ is the magnitude of the electron drift velocity parallel (−) or antiparallel (+) to $\vec{q}$, m_c is the cyclotron mass, and v_s is the velocity of sound. The period K_0 of the open orbit in $\vec{k}$ space can be related to $\langle v_q \rangle$, and hence can be expressed from Eq. (3) in terms of B_n^+ and B_n^- as

$$K_0 \cos\psi = (\pi ne/cq\hbar)(B_n^+ + B_n^-) \ , \qquad (4)$$

where ψ is the angle between $\vec{q}$ and the open direction in $\vec{r}$ space. Likewise, from Eq. (3), it follows that

$$m_c = (ne/2c\omega)(B_n^+ - B_n^-) \qquad (5)$$

and

$$\langle v_q \rangle = v_s[(B_n^+ + B_n^-)/(B_n^+ - B_n^-)] \ , \qquad (6)$$

so the cyclotron mass and drift velocity may in principle be determined simultaneously from the measured values of the resonance fields. In practice, however, $\langle v_q \rangle$ is usually too large to permit the Doppler splitting to be resolved, so m_c and $\langle v_q \rangle$ cannot be determined independently. Furthermore, the observed resonance peaks are the result of an integration over k_z [see Eq. (1)], so any values of m_c and $\langle v_q \rangle$ calculated from Eqs. (5) and (6) represent some sorts of averages for the entire open-orbit band. Finally, it can be shown[4] that the relative width of a particular resonance peak is determined only by the sound frequency, the velocity of sound, and the electron mean free path along $\vec{q}$. Then the mean free path l can be estimated from the relation[4]

$$l \simeq (2/q)[B_n/(\Delta B)_n] \ , \qquad (7)$$

where $(\Delta B)_n$ is the width of the nth resonance peak at the half-amplitude point.

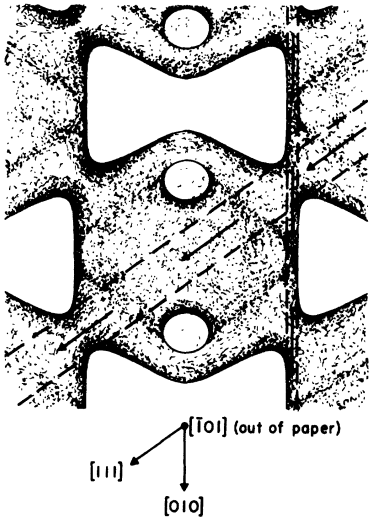

FIG. 1. Locations of the [111]- and [010]-directed open-orbit bands on the Fermi surface of copper (based on the model proposed in Ref. 11).

The degeneration of periodic open orbits into extended closed orbits is easily understood on the basis of a simplified model in which an open-orbit band is approximated by an infinitely long corrugated cylinder. The lengths L_k of the extended orbits formed as the magnetic field is rotated away from the plane perpendicular to the cylinder axis depend both on the angle of rotation $\Delta\theta_B$ and the diameter of the cylinder d_k:

$$L_k = d_k/\sin(\Delta\theta_B) \ . \qquad (8)$$

The matching of the orbit lengths in $\vec{r}$ space to the sound wavelength gives rise to the familiar magnetoacoustic oscillations which are periodic in $1/B$,

$$\Delta(1/B) = (2\pi e/cq\hbar)(1/L_k) \ , \qquad (9)$$

but which can occur at very high magnetic fields when the rotation angle is small.

III. EXPERIMENTAL PROCEDURE

The experiments were performed using a conventional pulse-echo technique,[12] where the relative attenuation of compressional waves was measured at a temperature of 4.2 °K in magnetic fields

up to 27 kG. All data presented here were taken on a single crystal of copper[3] having a resistivity ratio of 35 000, with the sound propagating along the $[\bar{1}01]$ crystal axis at frequencies from 11 to 53 MHz, and with $\vec{B}$ directed in the $(\bar{1}01)$ plane.

Since $ql \gg 1$ under these conditions, the attenuation proved to be extremely sensitive to small changes in the orientation of $\vec{B}$ relative to $\vec{q}$ and the crystal axes. To eliminate field-alignment errors, a sample holder was constructed which enabled the crystal to be tilted about two mutually perpendicular axes in the rotational plane of the magnet. With this system, $\vec{q}$ could be aligned perpendicular to the plane of rotation of $\vec{B}$ to within 0.1°, and the field could be set to within 0.03° of a given direction in the rotational plane. The criteria for determining when the crystal was properly aligned were based on an analysis of the symmetry of polar plots at high magnetic fields.

IV. RESULTS AND INTERPRETATION

A. Open-Orbit Resonances

The resonances caused by the [010]- and [111]-directed open-orbit bands with $\vec{B}$ parallel to [101] and $[1\bar{2}1]$, respectively, are compared in Fig. 2. The fundamental ($n = 1$) peak due to the [010] band is much broader and weaker than that due to the [111] band, and no Doppler-shift effect can be detected in either case. Furthermore, no harmonic ($n = 2, 3, \cdots$) peaks can be seen for the [010] resonance, the peaks appearing at lower fields being only magnetoacoustic oscillations from orbits of the "lemon" and "dog-bone" types. The absence of a Doppler effect indicates that the electron drift

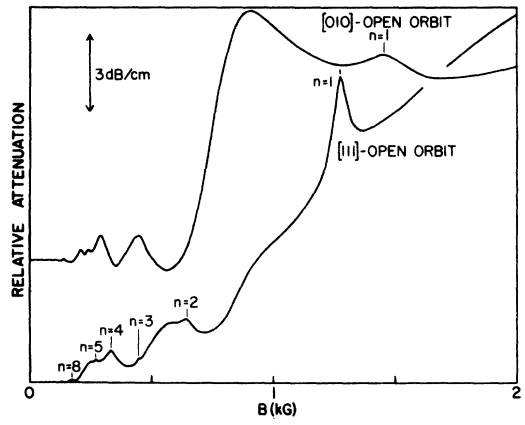

FIG. 2. Open-orbit resonances with $\vec{q} \parallel [\bar{1}01]$ and $f = 32.0$ MHz, superimposed on the low-field magnetoacoustic oscillations. The series of resonance peaks due to the [111]-directed orbits occurs when $\vec{B} \parallel [1\bar{2}1]$, and the single peak due to the [010]-directed orbits is found when $\vec{B} \parallel [101]$.

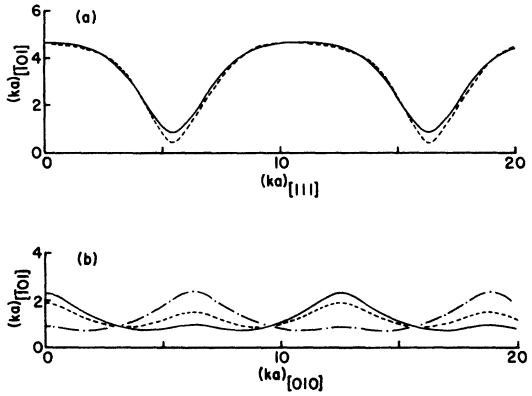

FIG. 3. Open orbits along [111] and [010] computed from the Halse-model Fermi surface. The cross sections of the [111] band (a) are at $(ka)_{[1\bar{2}1]} = 0$ (solid line) and $(ka)_{[1\bar{2}1]} = 0.8$ (broken line); while those of the [010] band (b) are at $(ka)_{[101]} = 4.3$ (solid line), $(ka)_{[101]} = 4.4$ (broken line), and $(ka)_{[101]} = 4.6$ (broken line with dots). Here $\vec{k}$ is the electron wave vector measured from the center of a zone, and a is the lattice constant.

velocities along both open-orbit bands are several orders of magnitude greater than the velocity of sound, i.e., $\langle v_q \rangle \gg v_s$. Some very weak harmonic peaks associated with the [010] open-orbit band were seen by Kamm[6] with $\vec{q} \parallel [\bar{1}11]$ and $\vec{B} \parallel [101]$ (in our coordinate system), so the failure to detect them here is probably due to the large background attenuation in this geometry.

Cross sections of the [111] and [010] open-orbit bands computed from a program[13] based on an analytic expression for the copper Fermi surface developed by Halse[11] are shown in Fig. 3. It is seen that the shape of the [010]-directed open orbits varies somewhat across the band, although the orbit period, being determined only by the Brillouin-zone dimension along [010] remains constant. The values of m_c and $\langle v_q \rangle$ computed from this model vary somewhat over both of the open-orbit bands. However, it can be concluded that electrons moving along the [010] open orbits have a larger average cyclotron mass (by about a factor of 3) and a correspondingly smaller average drift velocity along $\vec{q}$ than the electrons on the [111]-directed orbits.

In order to make a detailed study of the resonances, it is necessary to subtract the background due to other parts of the Fermi surface from the total attenuation, as illustrated in Fig. 4. Substitution of the magnetic field values at which the resonances occur into Eq. (4) (with $B_n^+ = B_n^-$ in this case) gives the values for the open-orbit periods listed in Table I, which are seen to agree within experimental error with the corresponding Brillouin-zone dimensions calculated from the value

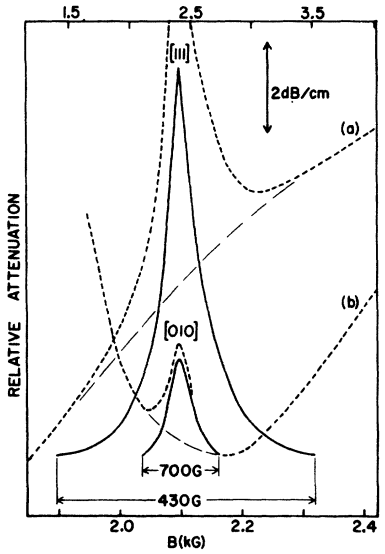

FIG. 4. Reduction of the open-orbit data by subtraction of an average background (long dashed line) from the recorded peaks (short dashed line). The bottom and top field scales are for the [111] (a) and [010] (b) peaks, respectively.

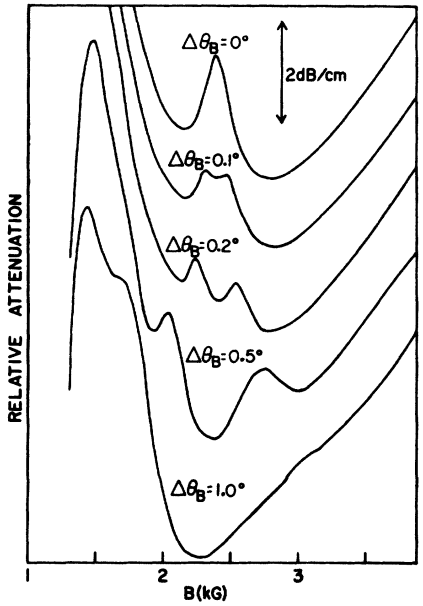

FIG. 5. Doppler splitting of the [010] open-orbit peak with rotation of $\vec{B}$ away from [101] in the $(\bar{1}01)$ plane. Here $f = 53.4$ MHz, and the curves are displaced arbitrarily in the vertical direction.

of the lattice constant at 0 °K.[14] Most of the uncertainty indicated for the values of K_0 is due to the approximately 1% uncertainty in the value of the ultrasonic frequency, which is a consequence[7] of the pulse-echo technique, and to a possible error of about 0.5%[6] in the velocity of sound. The greater uncertainty in the period of the [010]-directed open orbits is due to a less precise resolution of the resonance-field value.

Substitution into Eq. (7) of the relative resonance widths obtained from the reduced data of Fig. 4 yields the mean-free-path values listed in Table I. In this case, the indicated uncertainties are due to the arbitrariness involved in estimating the background attenuation. However, there may be an additional uncertainty in these l values due to an apparent broadening[7] of the resonance peaks

TABLE I. Open-orbit periods and mean-free-path values calculated from the resonance peaks caused by the [010]- and [111]-directed orbits.

Orbit direction	Field direction	K_0 (Å^{-1})	l (cm)
[010]	[101]	3.46 ± 0.05 (3.49^a)	0.032 ± 0.004
[111]	$[1\bar{2}1]$	3.03 ± 0.03 (3.02^a)	0.105 ± 0.008

[a]Corresponding Brillouin-zone dimension calculated from the lattice constant.

which can occur when the mean free path is of the same order of magnitude as the spatial extension of the ultrasonic wave packet. The fact that l for the [010]-directed orbits is smaller by about a factor of 3 than that for the [111]-directed orbits is probably due in large part to the smaller value of $\langle v_q \rangle$ for electrons on the [010] band, and so does not necessarily indicate a significant difference in relaxation times for the two orbits.

As $\vec{B}$ is rotated in the $(\bar{1}01)$ plane away from $[1\bar{2}1]$ or [101], the corresponding open orbits coalesce to form greatly extended closed orbits, but the open-orbit resonance peaks do not immediately disappear. In the case of the [111]-directed orbits, the resonance peaks broaden with field rotation but do not wash out completely until $\vec{B}$ is about 3° from $[1\bar{2}1]$. Evidently, resonant absorption of sound can continue as long as the electrons are able to satisfy Eq. (2) for a sufficient distance along the extended orbit.

The effect of field rotation in the case of the [010]-directed orbits is somewhat surprising. When $\vec{B}$ is rotated away from [101] by as much 0.1° (at 53.4 MHz), the [010] open-orbit resonance peak splits into two separate peaks, as shown in Fig. 5, and the splitting widens as the rotation angle is increased. If these two peaks are caused by the same resonance mechanism that gives rise to the single peak before rotation, then the effect can be explained in terms of a Doppler splitting. Applica-

TABLE II. Open-orbit period, drift velocity components, and cyclotron masses calculated from Doppler splitting of the [010] open-orbit resonance peak. Here $v_s = 5.08\times10^5$ cm/sec, $v_0 = 1.58\times10^8$ cm/sec, and $m_0 = 9.11\times10^{-28}$ g.

Angle of rotation of $\vec{B}$ [in $(\bar{1}01)$ plane] away from [101] (deg)	K_0 (Å^{-1})	$\langle v_q\rangle / v_s$	$\langle v_q\rangle / v_0$	m_c/m_0
0.10	3.46	30	0.096	4.2
0.22	3.46	16	0.051	7.9
0.48	3.47	7.4	0.024	17
1.0	3.45	3.8	0.012	33

tion of the formalism of Eqs. (4)–(6) to the resonance fields B_1^+ and B_1^- observed at each angle of rotation in Fig. 5 yields the values of open-orbit period, average cyclotron mass, and average drift-velocity component along $\vec{q}$ listed in Table II. The fact that the positions of the two peaks change with field direction in such a way as to maintain a constant value of K_0 from Eq. (4) is the most convincing evidence that Doppler splitting is taking place. The magnitude of the effect, however, is much greater than that observed in gallium,[9] where $\langle v_q\rangle$ was found to be about one-sixth of the free-electron Fermi velocity, and m_c turned out to be approximately equal to the free-electron mass. In the present case, it is found that by the time $\vec{B}$ is about 1° away from the symmetry axis $\langle v_q\rangle$ has dropped to one one-hundredth of the free-electron Fermi velocity, and m_c has risen to a value about thirty times greater than the free-electron mass

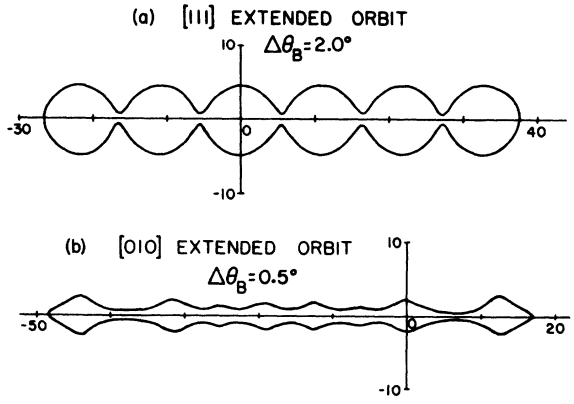

FIG. 6. Extended orbits formed from the [111]- and [010]-directed open orbits, as computed from the Halse-model Fermi surface. The cross section of the [111]-directed band (a) is at $(ka)_{\vec{B}} = 0.2$ with $\vec{B}$ rotated 2.0° from $[1\bar{2}1]$ in the $(\bar{1}01)$ plane, and that of the [010]-directed band (a) is at $(ka)_{\vec{B}} = 4.3$ with $\vec{B}$ rotated 0.5° from [101] in the $(\bar{1}01)$ plane. The scale is in units of ka.

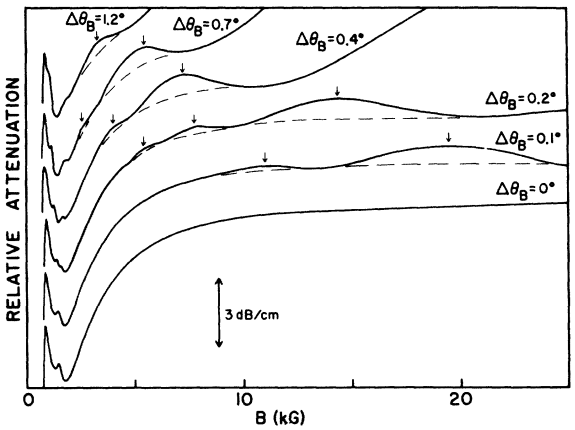

FIG. 7. High-field magnetoacoustic oscillations due to extended orbits formed from the [010]-directed open orbits as $\vec{B}$ is rotated away from [101] in the $(\bar{1}01)$ plane. The Doppler splitting of the open-orbit resonance peak can also be seen at lower fields. Here $f = 32.0$ MHz, and the curves are displaced arbitrarily in the vertical direction.

and six times greater than the maximum value[15] found for closed orbits (e.g., a four-Brillouin-zone extended orbit) by cyclotron resonance.

Typical extended orbits computed from the Halse-model Fermi surface with $\vec{B}$ near $[1\bar{2}1]$ and [101] are shown in Fig. 6. The relatively high degree of periodicity retained by orbits along the [111]-directed band can account for the persistence of the open-orbit resonance as the field is rotated away from $[1\bar{2}1]$. On the other hand, the apparent loss of periodicity with field rotation which takes place for orbits on the [010]-directed band would seem to preclude any open-orbit effects when $\vec{B}$ is no longer parallel to [101]. Likewise, the extreme values of m_c and $\langle v_q\rangle$ obtained from the Doppler-shift analysis cannot readily be explained on the basis of the Halse model. However, the shapes of the cross sections of the [010] band are quite sensitive to small deviations in the shape of the Fermi surface at the ends of the dog bone, so it is possible that small adjustments could be made in this region (without changing extremal dimensions) which would result in better agreement with the open-orbit data.

B. High-Field Magnetoacoustic Oscillations

The progression of the high-field magnetoacoustic oscillations with field rotation is illustrated in Fig. 7 for the case of the [010] band. The smallest field angle at which oscillations can be detected depends upon the sound frequency and the maximum obtainable field intensity; for example, when $f = 32.0$ MHz, the first oscillation peak appears at about 20 kG when $\vec{B}$ is 0.1° away from [101]. As $\Delta\theta_B$

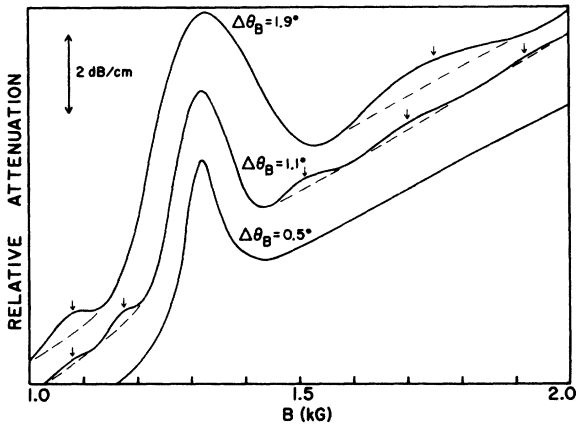

FIG. 8. High-field magnetoacoustic oscillations due to extended orbits formed from the [111]-directed open orbits as $\vec{B}$ is rotated away from [1$\bar{2}$1] in the ($\bar{1}$01) plane. The oscillations appear on both sides of the open-orbit resonance peak, which broadens with field rotation but does not exhibit Doppler splitting. Here $f = 33.5$ MHz, and the curves are displaced arbitrarily in the vertical direction.

TABLE III. Lengths of extended orbits in $\vec{k}$ space calculated from the periods of the high-field magnetoacoustic oscillations.

Orbit direction	Angle of rotation of $\vec{B}$ in ($\bar{1}$01) plane away from symmetry axis (deg)	L_k (Å^{-1})	Approximate number of Brillouin zones ($=L_k/K_0$)
~[010]	0.04	205	58.7
	0.09	88.6	25.3
	0.12	62.5	17.9
	0.18	41.7	12.0
	0.37	22.6	6.5
	0.57	15.5	4.4
	0.73	12.9	3.7
	1.20	9.7	2.8
~[111]	1.1	27.1	9.0
	1.9	14.3	4.7

increases, the lengths of the extended orbits decrease, so that the oscillations move to lower fields (and the splitting of the resonance peak begins). The sensitivity of the orbit lengths to field rotation depends upon the width of the band [see Eq. (8)] and is greater by about a factor of 4 for the [010] band than for the [111] band, as seen in Fig. 6.

The magnetoacoustic oscillations associated with the [111] extended orbits are more difficult to see at high fields because of the greater background attenuation for $\vec{B}$ near [1$\bar{2}$1]. However, for sufficiently large rotation angles, these oscillations show up clearly at lower fields, as seen in Fig. 8. The lengths of the extended orbits determined from the oscillation periods by Eq. (9) are listed in Table III, where it is seen that the longest orbit for which oscillations could be detected was along the [010] band and covered nearly 60 Brillouin zones. These values of L_k are found to be in close agreement with those computed from the Halse-Fermi surface, so the width of the [010] band appears to be given correctly by the Halse model.

V. CONCLUSIONS

A Doppler-shift analysis of the open-orbit resonance in copper with $\vec{B}$ near [101] indicates the possibility of extremely small electron drift velocities along the [010] band. Correspondingly, electrons moving along these orbits may have cyclotron masses which are an order of magnitude larger than the free-electron mass and so may be of great importance in any transport phenomena involving m_c.

High-field magnetoacoustic oscillations with $\vec{B}$ near [101] and [1$\bar{2}$1] indicate the presence of elongated closed orbits which can extend over many Brillouin zones. Such oscillations may be expected to appear in any metal when the field is near a direction giving rise to open-orbit resonance and must be taken into account when analyzing high-field attenuation data.

ACKNOWLEDGMENTS

We wish to express our appreciation to Dr. P. R. Antoniewicz for helpful discussions concerning data interpretation. We are grateful to Dr. L. T. Wood for the use of his computer program based on Dr. M. R. Halse's constants for the Fermi surface of copper which were kindly furnished us by Dr. D. Shoenberg. Our thanks also go to Dr. A. F. Clark for making the high-purity copper available and to S. J. Chang and J. P. Masson for their assistance with the experimental work.

†Work supported by a grant from the National Science Foundation.

[1]E. Fawcett, Advan. Phys. 13, 139 (1964).

[2]J. Mertsching, Phys. Status Solidi 37, 465 (1970), and references contained therein.

[3]Obtained from A. F. Clark, Natl. Bur. Std., Boulder, Colo.

[4]A. A. Galkin, E. A. Kaner, and A. P. Korolyuk, Dokl. Akad. Nauk SSSR 134, 74 (1960)[Soviet Phys. Doklady 5, 1002 (1961)]; A. A. Galkin, E. A. Kaner, and A. P. Korolyuk, Zh. Eksperim. i Teor. Fiz. 39, 1517 (1960)[Soviet Phys. JETP 12, 1055 (1961)].

[5]C. W. Burmeister, D. B. Doan, and J. D. Gavenda, Phys. Letters 7, 112 (1963).
[6]G. N. Kamm, Phys. Rev. B 1, 554 (1970).
[7]B. C. Deaton and J. D. Gavenda, Phys. Rev. 136, A1096 (1964).
[8]J. D. Gavenda and F. H. S. Chang, Phys. Rev. 186, 630 (1969).
[9]J. A. Munarin, Phys. Rev. 172, 737 (1968).
[10]J. R. Klauder, W. A. Reed, G. F. Brennert, and J. E. Kunzler, Phys. Rev. 141, 592 (1966).
[11]M. R. Halse, Phil. Trans. Roy. Soc. (London) A265, 507 (1969).
[12]J. D. Gavenda, in *Progress in Applied Materials Research*, edited by E. G. Stanford, J. H. Fearson, and W. J. McGonnagle (Heywood, London, 1964), Vol. 6, p. 43.
[13]L. T. Wood, Ph. D. thesis, University of Texas, 1968 (unpublished).
[14]D. Shoenberg, Phil. Trans. Roy. Soc. (London) A255, 98 (1963).
[15]J. F. Koch, R. J. Stradling, and A. F. Kip, Phys. Rev. 133, A240 (1964).

PHYSICAL REVIEW B VOLUME 3, NUMBER 2 15 JANUARY 1971

Many-Electron Correlation Effects on the Metallic Interionic Potential*

Wei-Mei Shyu
University of Hawaii, Honolulu, Hawaii 96822 *and Argonne National Laboratory, Argonne, Illinois* 60439

and

K. S. Singwi
Northwestern University, Evanston, Illinois 60204 *and Argonne National Laboratory, Argonne, Illinois* 60439

and

M. P. Tosi
Department of Physics, University of Messina, Messina, Italy
and Argonne National Laboratory, Argonne, Illinois 60439
(Received 31 August 1970)

The self-consistent treatment of electron correlations in the electron liquid recently given by Singwi *et al.* is applied to calculations of the interatomic force constants in alkali metals. With the Ashcroft form of the pseudopotential, in which the only parameter is the core radius, reasonably good agreement with the force constants derived from neutron inelastic scattering data is obtained, confirming the results of a previous analysis of the phonon dispersion curves. The longitudinal sound velocities for the three main symmetry directions are calculated in the same scheme. Results for the effective interionic potential are presented and discussed.

I. INTRODUCTION

The essential ingredients entering the estimation of the effective interionic potential in simple metals are the form of the pseudopotential and the treatment of the screening. Several forms of the pseudopotential are available – some of which include nonlocal corrections – as well as various forms of the screening function, ranging from simple Hartree screening to more complicated forms incorporating exchange and correlation effects. Recent work of Singwi, Sjölander, Tosi, and Land[1] has presented an improved self-consistent treatment of correlations in the homogeneous electron liquid, which yields a reasonably accurate dielectric function through the whole range of wave vector and electron density of interest in the theory of metals. This screening function has been used in calculations of the lattice dynamics of the alkali metals by Price, Singwi, and Tosi.[2] It was found that good agreement with the phonon dispersion curves, as determined by neutron inelastic scattering experiments,[3-6] could be obtained with the one-parameter local pseudopotential suggested by Ashcroft,[7] with values for the parameter which are in good agreement (for Na and K) or consistent (for Li and Rb) with those derived from Fermi-surface and liquid-resistivity data.

In this paper we consider again the information which can be extracted from the neutron scattering data. The emphasis is now put on the interionic potential in r space, which is the basic starting point for the study of other properties of metals, such as lattice defects and liquid dynamics. As is well known, the potential enters the lattice dynamics through interatomic force constants for various orders of neighbors, and these can be obtained from the phonon data by a Born–von Kàrmàn analysis. We analyze directly these force con-

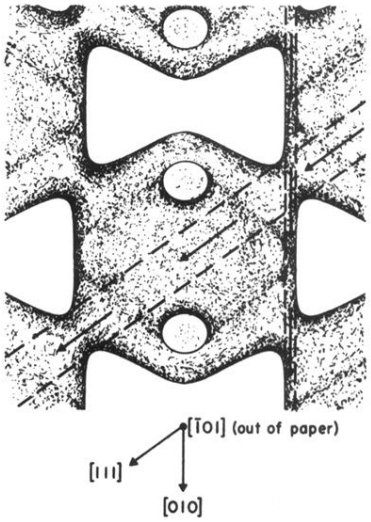

FIG. 1. Locations of the [111]- and [010]-directed open-orbit bands on the Fermi surface of copper (based on the model proposed in Ref. 11).